

## Angular distributions of specific gamma rays emitted in the deexcitation of prompt fission products of $^{252}\text{Cf}^\dagger$

A. Wolf\* and E. Cheifetz

Department of Nuclear Physics, Weizmann Institute of Science, Rehovot, Israel

(Received 5 February 1976)

Angular distributions of specific  $\gamma$  rays emitted in the deexcitation of prompt fission products of  $^{252}\text{Cf}$  were measured with respect to the fission direction. A total of 42 angular distributions were measured, 23 of which were of transitions in even-even fragments. The strong anisotropy ( $A_2=0.4-0.6$ ) measured for  $2^+ \rightarrow 0^+$ ,  $4^+ \rightarrow 2^+$ , and  $6^+ \rightarrow 4^+$  transitions in  $^{138,140}\text{Xe}$  and  $^{142,144}\text{Ba}$  provides direct evidence that the angular momentum of the primary fragments is completely aligned perpendicular to the fission axis. Most of the results are consistent with the results of a statistical calculation. The anisotropies measured for some transitions in even-odd fragments were combined with information of other authors in an attempt to determine spins of low-lying levels in these fragments. Finally, it is shown that about 60% of the anisotropy of the gross unresolved  $\gamma$ -ray spectrum, measured extensively by other authors, is due to transitions in the ground-state band of even-even fragments.

[ RADIOACTIVITY, FISSION  $^{252}\text{Cf}(sf)$ ; measured  $\sigma(\theta)$  of  $\gamma$  from fragments;  
Ge(Li) detector, 0.8 keV at 122 keV. ]

### I. INTRODUCTION

The angular distribution of  $\gamma$  rays emitted from the deexcitation of fission fragments is linked with the magnitude and alignment of the primary angular momentum of the fragments. These in turn are associated with certain vibrational modes such as bending, wriggling, or twisting of the nucleus at the saddle or scission points.<sup>1,2</sup> Most of the investigations in the past have dealt with the gross unresolved  $\gamma$  spectrum emitted by the fragments, which for spontaneous fission of  $^{252}\text{Cf}$  and thermal neutron induced fission of  $^{233,235}\text{U}$  and  $^{239}\text{Pu}$  (Refs. 3-11) has an anisotropy of  $N(0^\circ)/N(90^\circ) = 1.1-1.15$ , with respect to the fragment direction. Estimates for the magnitude of the angular momentum based on these results include many assumptions concerning the nature of the statistical deexcitation, the multipolarities of the transitions, and assumptions of average properties for the nucleus and the excited states contributing to the deexcitation process.

Angular distributions of specific  $\gamma$  rays from the spontaneous fission of  $^{252}\text{Cf}$  were measured by Wilhelmly *et al.*<sup>12</sup> In their work, the angular distributions of 13 specific transitions were determined, 7 of which were  $2^+ \rightarrow 0^+$  transitions in even-even nuclei, and the rest were transitions in even-odd and odd-odd nuclei. In the same work, the magnitude of the primary angular momentum of the fragments was inferred from the relative intensities of the ground-state band transitions of even-even fragments. The angular distributions of some of the  $2^+ \rightarrow 0^+$  transitions were found to be consistent

with the inferred magnitude of the primary angular momentum, and with the assumption of complete alignment of the primary angular momentum perpendicular to the fission direction.

In this work we present the results of a measurement of angular distributions of specific  $\gamma$  rays from the prompt deexcitation of fission fragments from spontaneous fission of  $^{252}\text{Cf}$ . A total of 42 angular distributions were measured, 23 of which were of transitions in even-even nuclei. In addition to  $2^+ \rightarrow 0^+$  transitions, we also measured the angular distributions of some  $4^+ \rightarrow 2^+$  and  $6^+ \rightarrow 4^+$  transitions, which provided further evidence for the assumption of complete alignment of the primary angular momentum.

The results of the angular distributions of the transitions in even-odd nuclei were used in an attempt to obtain spin assignments of low-lying states in  $^{105}\text{Mo}$  and  $^{111}\text{Ru}$ .

### II. EXPERIMENTAL TECHNIQUE AND ANALYSIS OF DATA

The experimental setup is shown schematically in Fig. 1. A  $10^7$  fissions/min  $^{252}\text{Cf}$  source, having an active radius of about 1 mm, was placed in an aluminum chamber together with three solid-state fission fragment detectors at  $45^\circ$  to each other and mounted on a single holder. The source was plated on a 25 mg/cm<sup>2</sup> copper backing in order to maintain the alignment of the angular momentum of the stopped fragments.  $\gamma$  rays from the fragments which stopped in the copper backing passed through a 7 mg/cm<sup>2</sup> aluminum window, and were detected by a 2 cm<sup>3</sup> planar, high resolution Ge(Li) detector.

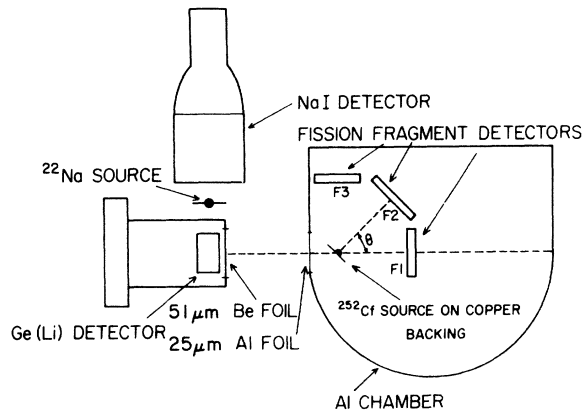


FIG. 1. Schematic description of the experimental setup. Relative distances and sizes of detectors are shown to scale.

This detector was placed outside the chamber at a distance of 5 cm from the source. In this arrangement, the source-Ge(Li) axis is kept fixed, and  $\gamma$  rays emitted from fragments stopped in the copper foil at three different angles with respect to the fission direction are measured simultaneously. The fission direction is defined by the complemen-

tary fission fragment which is detected in any one of the fission fragment detectors. The holder of the fission detectors was rotated by  $22.5^\circ$ , thus a total of six angles were measured:  $90^\circ$ ,  $67.5^\circ$ ,  $45^\circ$ ,  $22.5^\circ$ ,  $0^\circ$ , and  $-22.5^\circ$ . The distance of the fission fragment detectors from the source was about 3.5 cm and the solid angle subtended by each of them was 0.14 sr.

The alignment of the fission fragment detectors and the Ge(Li) detector with respect to the source was checked with a laser beam, and was accurate to  $1^\circ$ .

During the whole experiment the fission detectors were cooled to about  $-15^\circ\text{C}$  enabling them to withstand  $2 \times 10^9$  fragments (though with very poor kinetic energy resolution).

A three-parameter measurement was performed, in which the  $\gamma$ -ray energy in the range from 15–800 keV (8192 channels), the fission fragment kinetic energy, and the time difference between the detection of the fragment and the  $\gamma$  ray were measured and recorded on a magnetic tape. The time difference was measured with a time-to-amplitude converter, the start pulse being provided by a fast pulse derived from time pick-off units con-

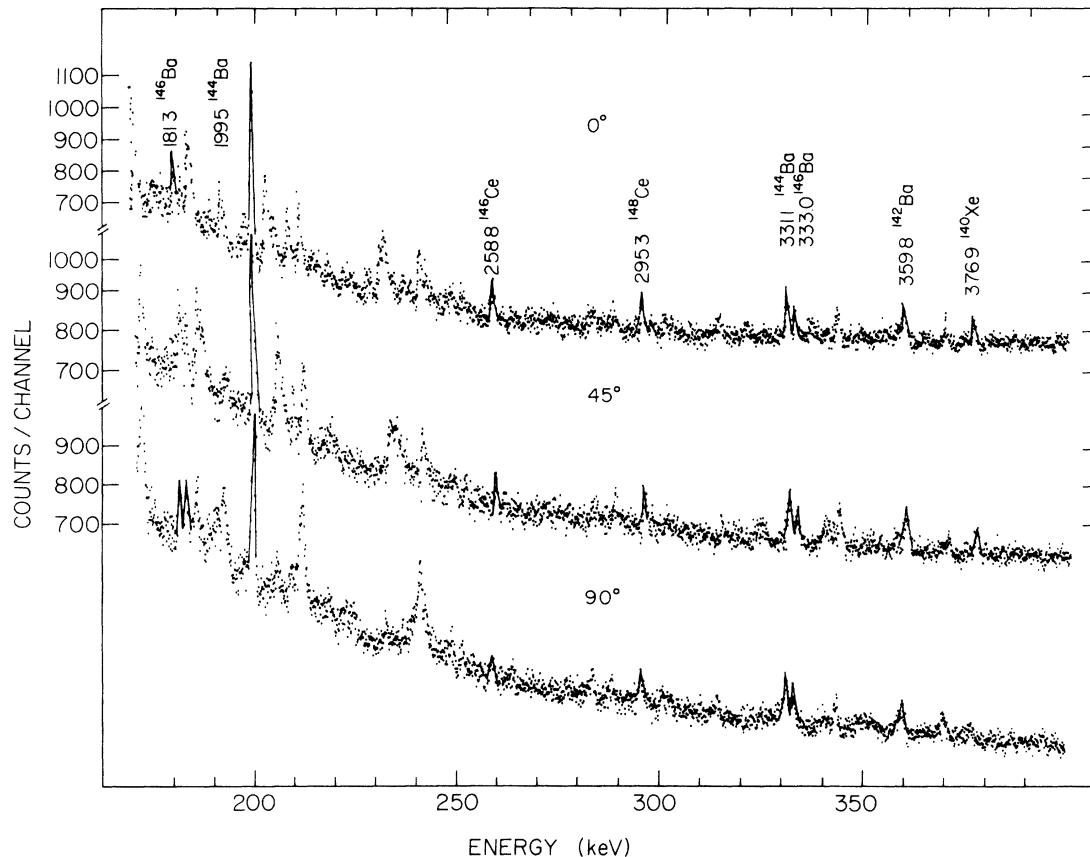


FIG. 2.  $\gamma$ -ray spectra emitted by heavy fragments at  $0^\circ$ ,  $45^\circ$ , and  $90^\circ$  with respect to the fission direction.

nected to each fission detector and the stop pulse given by a discriminator set on the leading edge of the  $\gamma$ -ray pulse.

A  $7.6 \times 7.6$  cm NaI detector together with a  $^{22}\text{Na}$  radioactive source were used in order to stabilize the  $\gamma$ -ray detection system. Whenever a coincidence event occurred between two 511 keV  $\gamma$  rays which were detected in the Ge(Li) detector and the NaI detector, respectively, a gate pulse was produced by a fast-slow coincidence system which triggered the operation of a digital gain stabilizer. The rate of stabilization events was about 17 per minute and was found to be satisfactory. Each multidimensional event was also characterized by several bits of information specifying which fission detector was involved, or whether it was a stabilization event. The data were later processed at the IBM 370/165 computer center of the Weizmann Institute.

The timing resolution after correcting in the computer analysis for the experimental walk varied from about 10 nsec full width at half maximum (FWHM) at  $\gamma$  energies of 100 keV, to about 6.5 nsec at 500 keV.

For each fission fragment detector, i.e., for each angle, the events were sorted according to whether the fragment was light or heavy, and in

10 time intervals from -14 to 2600 nsec. Thus, 20  $\gamma$  spectra, 8192 channels each, were obtained for each angle. (In this experiment only light-heavy fragment identification was obtained, as the kinetic energy of only one fragment was measured.)

In Fig. 2 we present a portion of the spectra obtained at three angles, when the heavy fragment stopped in the copper backing, for the time interval -14 to 44 nsec (prompt spectra). The energy resolution varied from 0.8 keV (FWHM) at 100 keV, to 1.3 keV at 600 keV. The  $\gamma$ -ray spectra were analyzed by using the SAMPO computer code.<sup>13</sup>

In this paper we will discuss only the results concerning prompt radiation (the time interval -14 to 44 nsec).

### III. RESULTS

The assignment of the different  $\gamma$  rays to specific fragments was made by comparing their energies and intensities with the works of Cheifetz *et al.*,<sup>14</sup> Cheifetz and Wilhelmy,<sup>15</sup> John, Guy, and Wesolowski,<sup>16</sup> and Clark, Glendenin, and Talbert.<sup>17</sup> The energies differed in most cases by not more than 0.1 keV. The differentiation between light and heavy fragments provided a further check on the correct identification. Most of the strong lines

TABLE I. Angular distribution coefficients and intensities of  $\gamma$  transitions in even-even fragments.

Isotope	$E_\gamma$ (keV)	Transition	Present work		Wilhelmy <i>et al.</i> (Ref. 12)		Photons/fission (% error)
			$A_2$	$A_4$	$A_2$	$A_4$	
$^{100}\text{Zr}$	212.7	$2^+ \rightarrow 0^+$	$0.26 \pm 0.04$	$0.02 \pm 0.05$			0.015(14)
$^{100}\text{Zr} + ^{95}\text{Sr}^a$	352.2	$4^+ \rightarrow 2^+$	$0.27 \pm 0.07$	$-0.17 \pm 0.10$			0.016(17)
$^{102}\text{Zr}$	152.0	$2^+ \rightarrow 0^+$	$0.24 \pm 0.03$	$-0.23 \pm 0.05$			0.013(15)
	326.6	$4^+ \rightarrow 2^+$	$0.25 \pm 0.08$	$-0.35 \pm 0.18$			0.010(25)
$^{104}\text{Mo}$	192.5	$2^+ \rightarrow 0^+$	$0.15 \pm 0.03$	$0.00 \pm 0.03$	$0.27 \pm 0.12$	$0.07 \pm 0.22$	0.031(10)
	368.8	$4^+ \rightarrow 2^+$	$0.21 \pm 0.09$	$-0.17 \pm 0.13$			0.018(20)
$^{106}\text{Mo}$	171.9	$2^+ \rightarrow 0^+$	$0.13 \pm 0.04$	$0.04 \pm 0.04$	$0.07 \pm 0.10$	$0.06 \pm 0.15$	0.033(13)
	350.9	$4^+ \rightarrow 2^+$	$0.52 \pm 0.09$	$-0.06 \pm 0.10$			0.016(15)
$^{108}\text{Ru}$	242.4	$2^+ \rightarrow 0^+$	$0.19 \pm 0.03$	$0.20 \pm 0.04$			0.019(15)
$^{110}\text{Ru}$	240.9	$2^+ \rightarrow 0^+$	$0.11 \pm 0.02$	$0.06 \pm 0.03$	$0.23 \pm 0.10$	$0.20 \pm 0.15$	0.036(13)
$^{108}\text{Ru} + ^{110}\text{Ru}^b$	423.1	$4^+ \rightarrow 2^+$	$0.22 \pm 0.08$	$-0.52 \pm 0.12$			0.022(20)
$^{138}\text{Xe}$	589.1	$2^+ \rightarrow 0^+$	$0.49 \pm 0.13$	$-0.21 \pm 0.16$			0.021(20)
$^{140}\text{Xe}$	376.9	$2^+ \rightarrow 0^+$	$0.61 \pm 0.11$	$-0.24 \pm 0.12$			0.016(17)
	457.8	$4^+ \rightarrow 2^+$	$0.46 \pm 0.12$	$0.07 \pm 0.15$			0.013(17)
$^{142}\text{Ba}$	359.8	$2^+ \rightarrow 0^+$	$0.45 \pm 0.09$	$-0.15 \pm 0.11$			0.021(18)
	475.6	$4^+ \rightarrow 2^+$	$0.13 \pm 0.12$	$0.17 \pm 0.16$			0.015(20)
$^{144}\text{Ba}$	199.5	$2^+ \rightarrow 0^+$	$0.24 \pm 0.02$	$0.05 \pm 0.02$	$0.20 \pm 0.10$	$-0.06 \pm 0.15$	0.032(10)
	331.1	$4^+ \rightarrow 2^+$	$0.30 \pm 0.04$	$-0.10 \pm 0.06$			0.027(15)
	431.6	$6^+ \rightarrow 4^+$	$0.43 \pm 0.11$	$-0.13 \pm 0.14$			0.017(20)
$^{146}\text{Ba}$	181.3	$2^+ \rightarrow 0^+$	$0.21 \pm 0.05$	$-0.40 \pm 0.09$			0.007(20)
$^{146}\text{Ba} + ^{114}\text{Pd}^c$	333.0	$4^+ \rightarrow 2^+; 2^+ \rightarrow 0^+$	$0.22 \pm 0.05$	$-0.08 \pm 0.08$			0.013(20)
$^{146}\text{Ce}$	258.8	$2^+ \rightarrow 0^+$	$0.38 \pm 0.10$	$0.22 \pm 0.13$			0.007(20)
$^{148}\text{Ce}$	295.3	$4^+ \rightarrow 2^+$	$0.26 \pm 0.08$	$-0.05 \pm 0.11$			0.018(18)

<sup>a</sup> 80% of the intensity of this line is due to the  $4^+ \rightarrow 2^+$  transition in  $^{100}\text{Zr}$  (Ref. 14).

<sup>b</sup> 60% of the intensity of this line is from  $^{110}\text{Ru}$  (Ref. 14).

<sup>c</sup> 50% of the intensity of this line is due to the  $2^+ \rightarrow 0^+$  transition in  $^{114}\text{Pd}$ , which was not completely eliminated by the light-heavy differentiation because of the poor kinetic energy resolution of the fission detectors.

seen in the spectra are emitted in the deexcitation of even-even fragments and are associated with the ground-state band.<sup>14</sup> In fact, most of the results presented below refer to  $2^+ \rightarrow 0^+$  and  $4^+ \rightarrow 2^+$  transitions. The level schemes and the spin assignments were made by Cheifetz *et al.*<sup>14</sup>

The angular distribution is expanded as usual in the form:

$$W(\theta) = a_0 + a_2 P_2(\cos\theta) + a_4 P_4(\cos\theta).$$

The coefficients  $a_0$ ,  $a_2$ , and  $a_4$  were determined by a least-squares procedure. The parameters  $A_2 = a_2/a_0$  and  $A_4 = a_4/a_0$  and the photon yields are given in Table I for all the transitions in even-even nuclei measured in this work. For comparison, the results of Wilhelmy *et al.*<sup>12</sup> are also presented in Table I. The results of the experiments are in agreement within the experimental errors, with the exception of the 212.7 keV  $2^+ \rightarrow 0^+$  transition in <sup>100</sup>Zr. In this case only four angles were measured in the work of Wilhelmy *et al.*, and this may be the reason for the discrepancy. It should also be noted that in our experiment a copper backing was used, while Wilhelmy *et al.* used a platinum backing. In principle this may also cause some difference between the results, because of extranuclear effects which could be different in different hosts. However, the difference is not expected to be important, as long as short-lived ( $t_{1/2} < 10$  nsec) transitions are involved.

The photon yields given in Table I are consistent with the results of Cheifetz *et al.*,<sup>14</sup> when corrected for internal conversion.

In addition to the results given in Table I, 19

other angular distributions were measured; several of these transitions could be assigned to specific even-odd or odd-odd fragments. The rest could not be unambiguously identified, and we can specify only whether they were emitted by a light or heavy fragment. Further work in this field may possibly add information regarding the unassigned transitions.

The angular distribution coefficients for these transitions are given in Table II. Again, it is seen that our results are in agreement with those of Wilhelmy *et al.* (within the experimental errors) with the exception of the 91.6 keV transition in <sup>107</sup>Tc. The reason for this discrepancy is not clear.

Most of the transitions listed in Table II are seen to have negative values of  $A_2$  (i.e., the intensity increases towards 90°). As we shall see in the next section, this is connected with the fact that half-integral spins are involved, and a  $M1 + E2$  mixture is possible.

In Fig. 3 we present some of the angular distributions measured in this work.

#### IV. DISCUSSION

##### A. Transitions in even-even nuclei

The  $A_2$  coefficients of the angular distributions of  $2^+ \rightarrow 0^+$  and  $4^+ \rightarrow 2^+$  transitions in even-even fragments are plotted as a function of mass number in Figs. 4 and 5. A systematic behavior is observed. In order to explain this behavior the procedure described by Wilhelmy *et al.*<sup>12</sup> can be used, in which the angular distribution coefficients are

TABLE II. Angular distribution coefficients and intensities of  $\gamma$  transitions in other nuclei.

Isotope	$E_\gamma$ (keV)	Present work		Wilhelmy <i>et al.</i>		Photons/fission (% error)
		$A_2$	$A_4$	$A_2$	$A_4$	
<sup>95</sup> Sr	204.4	0.75 ± 0.10	0.19 ± 0.13			0.005(20)
<sup>101</sup> Zr + <sup>109</sup> Ru	98.3	-0.35 ± 0.02	-0.01 ± 0.03	-0.32 ± 0.09	-0.10 ± 0.13	0.012(15)
<sup>105</sup> Mo	94.9	-0.30 ± 0.02	-0.09 ± 0.02	-0.21 ± 0.09	-0.20 ± 0.13	0.015(15)
( <sup>107</sup> Tc) ( <sup>101</sup> Zr)	91.6	0.35 ± 0.08	-0.03 ± 0.08	0.08 ± 0.09	-0.19 ± 0.14	0.005(17)
<sup>108</sup> Tc	138.4	-0.13 ± 0.04	-0.08 ± 0.05	-0.08 ± 0.10	0.11 ± 0.15	0.017(15)
<sup>109</sup> Tc	119.5	0.09 ± 0.04	-0.07 ± 0.06			0.007(17)
<sup>109</sup> Ru	132.1	-0.05 ± 0.05	-0.06 ± 0.07			0.005(18)
<sup>111</sup> Ru	104.1	0.03 ± 0.03	0.18 ± 0.04	0.15 ± 0.10	-0.06 ± 0.15	0.007(15)
<sup>111</sup> Ru	150.4	-0.15 ± 0.05	-0.08 ± 0.06			0.014(15)
Light	122.1	0.33 ± 0.14	-0.22 ± 0.13			0.004(18)
Light	125.4	-0.05 ± 0.05	-0.05 ± 0.07			0.012(15)
Light	126.1	-0.02 ± 0.05	0.01 ± 0.07			0.012(15)
Light	134.0	-0.08 ± 0.08	-0.07 ± 0.10			0.004(20)
Light	142.6	-0.01 ± 0.04	0.07 ± 0.07			0.006(17)
Light	144.9	-0.16 ± 0.04	-0.18 ± 0.07			0.008(18)
<sup>134</sup> I	182.9	-0.10 ± 0.08	-0.32 ± 0.14			0.006(25)
<sup>143</sup> Ba	117.6	-0.20 ± 0.04	0.12 ± 0.05			0.016(12)
Heavy	112.8	-0.44 ± 0.05	0.17 ± 0.06			0.009(16)
Heavy	343.4	0.36 ± 0.09	-0.10 ± 0.12			0.019(17)

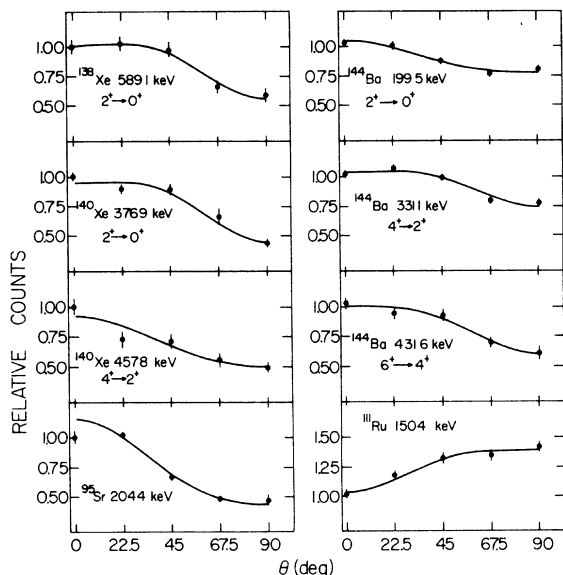


FIG. 3. Angular distributions of several transitions measured in this work. The solid lines were obtained by a least-squares-fitting procedure to  $W(\theta) = a_0[1 + A_2 P_2(\cos\theta) + A_4 P_4(\cos\theta)]$ .

calculated by assuming that the angular momentum of the fragments is initially completely aligned perpendicular to the fission axis. In the calculation, the relative population of the magnetic substates is being followed, first during the neutron evaporation, and subsequently through the statistical emission of a number of  $E1$   $\gamma$  rays and then during the cascade of the ground-state band. From such a calculation, the relative population of the substates and the states themselves are obtained and can be used to derive the angular distribution

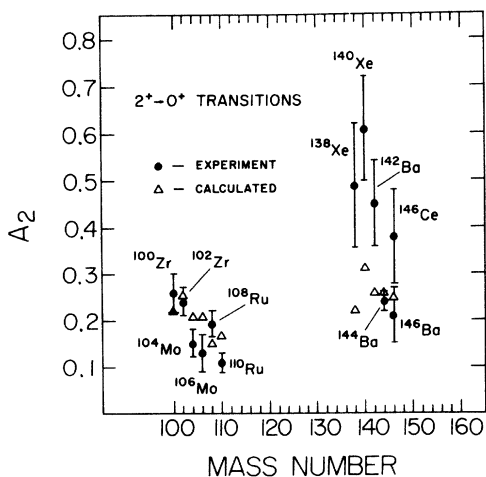


FIG. 4. Angular distribution coefficients  $A_2$  of  $2^+ \rightarrow 0^+$  transitions as a function of the mass number of the fragment. Dots denote experimental values; triangles denote values calculated by Wilhelmy (Ref. 20).

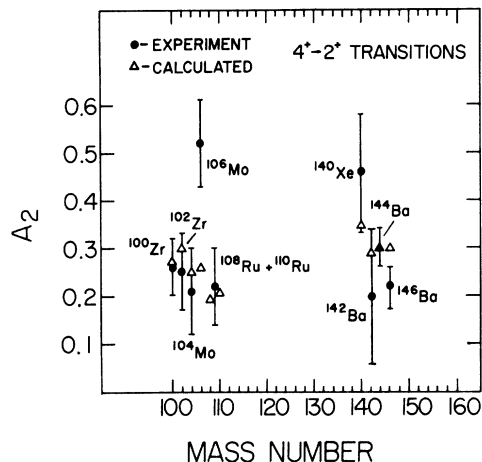


FIG. 5. Angular distribution coefficients  $A_2$  of  $4^+ \rightarrow 2^+$  transitions as a function of the mass number of the fragment.

coefficients. The parameters in the calculation are as follows:

- The number of neutrons evaporated, which is taken from the experimental average number of neutrons emitted as a function of fragment mass.
- The spin cut-off parameters for the fragments during the process, which is estimated<sup>18</sup> from measurements of isomeric yield ratios in neutron capture and charged particle reactions.
- The number  $n_\gamma$  of  $E1$   $\gamma$  rays emitted before reaching the state in question. In the work of Wilhelmy *et al.*<sup>12</sup> it was assumed that  $n_\gamma = 3$ . This assumption was based on the measured<sup>19</sup> average number of  $\gamma$  rays associated with the prompt de-excitation process.
- The rms value of the primary angular momentum of the fragments, which was determined by Wilhelmy *et al.*,<sup>12</sup> using (a), (b), and (c) so as to fit best the relative intensities of the observed ground-state-band transitions.

The anisotropy of the angular distribution decreases with the increase of both the number of neutrons and the number of statistical  $\gamma$  rays emitted, as these tend to disperse the original direction of the angular momentum. The values of  $A_2$  calculated by Wilhelmy<sup>20</sup> following the above procedure are also plotted in Figs. 4 and 5 and are seen to be in reasonable agreement with the experimental results, with the exception of the <sup>138,140</sup>Xe and <sup>142</sup>Ba isotopes. The experimental fact that the  $4^+ \rightarrow 2^+$  transitions have a more anisotropic angular distribution than the  $2^+ \rightarrow 0^+$  transitions is reproduced by the calculation. The calculated values of  $A_4$  are between  $(-0.12) - (+0.04)$  and are usually negative. This is in general agreement with the results presented in Table I. (See also average  $A_4$  values in Table III.)

TABLE III. Average angular distribution coefficients and relative yields of transitions in the ground-state bands of even-even fragments.

Transition	$A_2$	$A_4$	Relative yield <sup>a</sup>
$2^+ \rightarrow 0^+$	0.26	-0.03	100
$4^+ \rightarrow 2^+$	0.29	-0.14	68
$6^+ \rightarrow 4^+$	0.43	-0.15	35
$8^+ \rightarrow 6^+$ <sup>b</sup>	0.43	-0.15	15

<sup>a</sup> The relative yields were taken as the average of the photon yields for all known transitions in even-even fragments (Ref. 14).

<sup>b</sup> Angular distributions were not measured, therefore  $A_2$  and  $A_4$  were assumed to be the same as for  $6^+ \rightarrow 4^+$  transitions. For a completely aligned  $8^+$  state, the calculated (Ref. 20) values are  $A_2=0.43$  and  $A_4=-0.20$ .

The very high anisotropy found in the  $^{138,140}\text{Xe}$  and  $^{142}\text{Ba}$  isotopes is probably due to the fact that in these isotopes the  $4^+$  states are rather high (at about 1 MeV) and therefore the ground-state band is reached either directly after the neutron evaporation, or after emission of less than the assumed three  $E1$   $\gamma$  rays. This argument is illustrated in Fig. 6, where the  $A_2$  coefficients of  $2^+ \rightarrow 0^+$  transitions are plotted as a function of the energy of the  $4^+$  state. There is a correlation between the values of  $A_2$  and  $E(4^+)$ , with a correlation coefficient of  $\rho=0.75$  and a significance level of less than 0.5%.

The value of  $A_2$  was calculated<sup>20</sup> for various numbers of  $E1$   $\gamma$  rays,  $n_\gamma$ , preceding the ground-state band, and it was found that  $A_2$  decreases by about 10% for each  $E1$   $\gamma$  ray. This gives a maximum value of  $A_2=0.40$  for the case  $n_\gamma=0$ , which is closer to the experimental values for the three

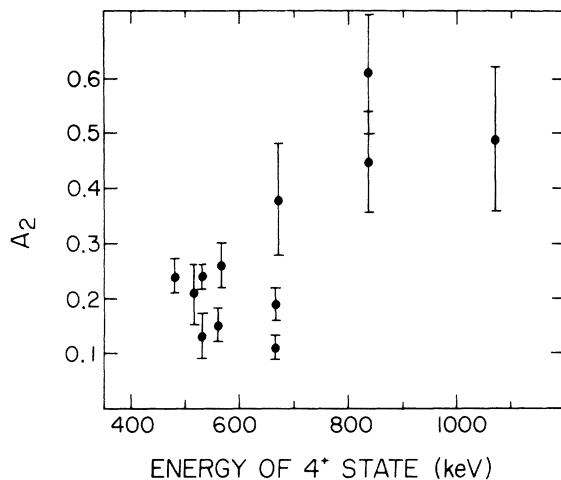


FIG. 6. Angular distribution coefficients  $A_2$  of  $2^+ \rightarrow 0^+$  transitions vs the energy of the  $4^+$  state in the respective isotope.

isotopes in question. The presence of any non-stretched  $E2$  transitions is not probable, since they cause<sup>21</sup> a more drastic decrease in anisotropy than  $E1$  transitions.

Here it should be pointed that the angular distributions of the  $\gamma$  rays in a stretched  $E2$  cascade of the form  $J \rightarrow J-2 \rightarrow \dots \rightarrow 4 \rightarrow 2 \rightarrow 0$  are the same for all the transitions,<sup>21</sup> and depend only on the initial spin  $J$  and the degree of alignment of the initial state. For a completely aligned  $J=6$  state,<sup>21</sup>  $A_2=0.45$  and  $A_4=-0.24$  for all the  $\gamma$  rays of the cascade. These values are very close to the results for the  $4^+ \rightarrow 2^+$  and  $2^+ \rightarrow 0^+$  transitions in  $^{138,140}\text{Xe}$  and  $^{142}\text{Ba}$  and the result for the  $6^+ \rightarrow 4^+$  transition in  $^{144}\text{Ba}$  (see Table I). In this last case, the angular distributions of three transitions were measured:  $6^+ \rightarrow 4^+$ ,  $4^+ \rightarrow 2^+$ , and  $2^+ \rightarrow 0^+$ . The yields of these transitions are different and clearly indicate that only about 46% of the  $2^+ \rightarrow 0^+$  transition and 62% of the  $4^+ \rightarrow 2^+$  transition are fed via the  $6^+ \rightarrow 4^+$  transition (see Table I). To obtain the above results, the yields of Table I were corrected for internal conversion.<sup>22</sup> If one assumes that the respective parts of the  $4^+ \rightarrow 2^+$  and  $2^+ \rightarrow 0^+$  transitions which are not from the stretched cascade have an isotropic angular distribution, then the value of  $A_2=0.43$  for the  $6^+ \rightarrow 4^+$  transition implies values of  $A_2=0.27$  and  $A_2=0.20$  for the  $4^+ \rightarrow 2^+$  and  $2^+ \rightarrow 0^+$  transitions, respectively. These values are somewhat lower than the experimental results, indicating that the transitions which are not fed via the  $6^+$  state are also somewhat anisotropic. The same analysis, based on the yields of the  $4^+ \rightarrow 2^+$  and  $2^+ \rightarrow 0^+$  transitions and corrected for electron conversion, was applied in all the other cases of Table I, and the angular distributions were found to be consistent within the experimental errors.

One interesting conclusion from the above discussion is connected to the alignment of the angular momentum of the primary fragments. As was mentioned before, the statistical calculation of Wilhelmy *et al.*<sup>12</sup> starts with the basic assumption of complete alignment of the primary fragments in a direction perpendicular to the fission axis. This assumption implies that the vibrational modes<sup>2</sup> of bending and wriggling at the scission point (with perhaps subsequent Coulomb excitation) are dominant in their contribution to the primary angular momentum of the fragments, whereas any twisting mode (of one fragment with respect to the other) is negligible. As was shown above most of the calculated anisotropies follow closely the experimental results, thus indicating the validity of the basic assumption. Moreover, in several cases (i.e.,  $^{138,140}\text{Xe}$ , and  $^{142,144}\text{Ba}$ ) the angular distributions of the transitions in the stretched cascades were found to be very close to those expected

from completely aligned states. This may be considered a direct evidence that the primary fragments are formed with the angular momentum completely aligned perpendicular to the fission axis, since the evaporation of one or two neutrons can only cause dealignment.

#### B. Transitions in other nuclei

The prompt  $\gamma$  spectrum also contains contributions from the deexcitation of even-odd and odd-odd nuclei. In these cases the decay scheme of even the low-lying states is in general more complicated than for the even-even nuclei. Therefore, when intense lines associated with such nuclei are observed, it may be concluded that they are associated with low-lying states.

We shall attempt in the following to combine the data obtained previously by other methods with our angular distribution results in order to obtain spectroscopic information regarding even-odd nuclei. Whereas in the even-even nuclei the transitions measured were  $E2$  transitions between states of known spin and parity, in the even-odd cases the spins of the states are not known. In principle, the angular distribution results can provide some information regarding the spins. The angular distribution coefficients  $A_2$  and  $A_4$  depend on<sup>23</sup>:

- (1) the initial and final spins,
- (2) the multipolarities and mixing ratio ( $\delta$ ) of the transitions, and
- (3) the relative population of the magnetic substates of the initial state.

The values of  $A_2$  and  $A_4$  were calculated for various transitions following the formulas of de Groot,<sup>23</sup> for different mixing ratios ( $\delta$ ). We assumed a Gaussian distribution (normalized between  $\pm J$ ) for the population of the magnetic substates, centered at  $m=0$  with different standard deviations ( $\sigma$ ).

Two cases are discussed below.

#### 94.9 keV transition in <sup>105</sup>Mo

Information concerning this transition was obtained from electron conversion studies by Watson *et al.*<sup>24</sup> who reported a half-life of 1.1 nsec and a  $K/L$  ratio of 4.8, consistent with a predominantly  $E2$  transition. The photon yield of this transition was found to be 1.5% per fission (Table II); after correction for  $E2$  electron conversion, a total yield of 3.8% per fission is obtained. The independent yield of <sup>105</sup>Mo is 4.3% per fission. Therefore about 90% of the transitions leading to the ground state of <sup>105</sup>Mo are via the 95 keV line. Such concentration of strength has otherwise been observed<sup>14</sup> only in the  $2^+ \rightarrow 0^+$  transitions to ground state of even-even products, and therefore it may be concluded that the 95 keV line leads to the

ground state of <sup>105</sup>Mo.

The spin of the ground state of <sup>105</sup>Mo can be inferred from the Nilsson diagrams assuming the deformation parameter  $|\beta|=0.33$  obtained by Jared, Nifenecker, and Thompson<sup>25</sup> from direct lifetime measurements of the  $2^+ \rightarrow 0^+$  transitions in the adjacent <sup>104,106</sup>Mo isotopes. The most probable Nilsson configurations<sup>26</sup> are either  $\frac{5}{2}^- [532]$  for a prolate deformation or  $\frac{5}{2}^+ [402]$  for an oblate deformation.

The first excited state at 95 keV decaying predominantly by  $E2$  radiation<sup>24</sup> to the  $\frac{5}{2}$  ground state may have one of the following spins:  $\frac{1}{2}$ ,  $\frac{3}{2}$ ,  $\frac{5}{2}$ ,  $\frac{7}{2}$ , and  $\frac{9}{2}$ . For  $J=\frac{1}{2}$ , the angular distribution is isotropic. For  $J=\frac{9}{2}$ , the values of  $A_2$  are positive for all possible values of  $\sigma$  (the standard deviation of the magnetic substates population distribution). The values of  $A_2$  as a function of  $\delta$  ( $E2/M1$  mixing ratio) and plausible values of  $\sigma$  are shown in Fig. 7 for the spin values  $\frac{3}{2}$ ,  $\frac{5}{2}$ , and  $\frac{7}{2}$ . The experimental value of  $A_2$  is  $-0.30 \pm 0.03$  (see Table II and Fig. 7). It is clearly inconsistent with  $J=\frac{1}{2}$  or  $J=\frac{9}{2}$ . The most reasonable values of  $A_2$  that are consistent with a large  $\delta$  (we estimate  $|\delta| > 1.7$  from the work of Watson *et al.*<sup>24</sup>) are seen in Fig. 7 to correspond to  $J=\frac{5}{2}$  or  $J=\frac{7}{2}$  and values of  $\sigma$  between 1–2. These values of  $\sigma$  are reasonable if one takes into consideration the dealignment caused by previous decays. The value  $J=\frac{3}{2}$  cannot be excluded, since for a large value of  $\sigma$  ( $\sigma > 2.5$ , i.e.,

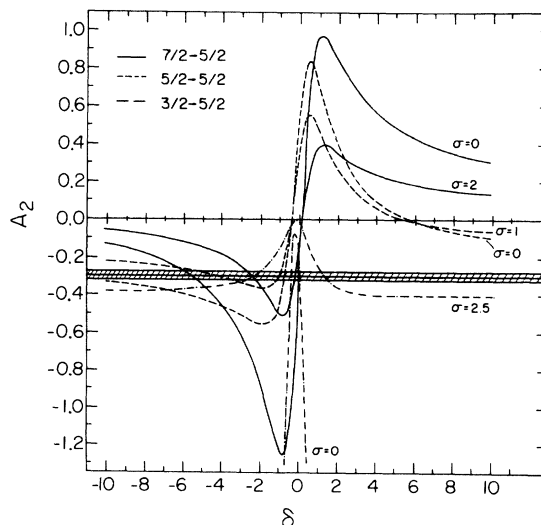


FIG. 7. Dependence of the angular distribution coefficient  $A_2$  on the multipolarity mixing ratio  $\delta(E2/M1)$ , for different values of  $\sigma$  (the standard deviation of the magnetic substates population), and different spin sequences possible for the 95 keV transition in <sup>105</sup>Mo. The experimental value is shown as a shaded rectangle.

very weak alignment) it may also fit the observed anisotropy.

In conclusion, although the 95 keV line is the strongest transition assigned to an even-odd prompt product and has a clear anisotropy, the combined results of angular distribution and electron conversion measurements are insufficient for a unique determination of the spins involved. On the basis of the information presented here and a model dependent assignment of the ground-state spin, possible values of the spin of the excited state in question are  $\frac{7}{2}$ ,  $\frac{5}{2}$ , (less likely)  $\frac{3}{2}$ , leading to a  $\frac{5}{2}$  ground state.

#### Transitions in the $^{111}\text{Ru}$ isotope

The angular distributions of two transitions in this isotope were measured, namely, 104.1 keV with  $A_2 = 0.03 \pm 0.03$  and 150.4 keV with  $A_2 = -0.15 \pm 0.05$ . A decay scheme of  $^{111}\text{Ru}$  was proposed by Cheifetz *et al.*,<sup>27</sup> based on  $\gamma$ - $\gamma$  coincidence measurements. According to this scheme, the first excited state is 104.0 keV. Therefore, in this case we can use similar considerations as above for the 104.1 keV line.

The possible Nilsson configurations in this case are  $\frac{1}{2}^+[420]$  or  $\frac{1}{2}^+[411]$  for a deformation  $|\beta| = 0.3$  inferred from the work of Jared *et al.*<sup>25</sup>

In this case there is no information about the  $K/L$  electron conversion ratio. The possible spin values for the 104.1 keV level are  $\frac{1}{2}$ ,  $\frac{3}{2}$ , and  $\frac{5}{2}$ . For a  $\frac{5}{2} \rightarrow \frac{1}{2}$  transition, an  $A_2$  value consistent with the experimental result may be obtained only for a very weak alignment ( $\sigma > 3$ ). Therefore in this case, the more probable value of the spin of the first excited state is either  $\frac{1}{2}$  or  $\frac{3}{2}$ , both of which may give an isotropic angular distribution. As in the previous case, this conclusion is based on the model dependent assignment of the ground-state spin.

#### C. Gross anisotropy of $\gamma$ rays

Although our results were obtained for specific transitions, their average features enable us to understand the anisotropy of the gross unresolved  $\gamma$ -ray spectrum. All the transitions of Table I, which are associated with even-even fragments, have a positive  $A_2$  value with an average of 0.27, which corresponds to a  $W(0^\circ)/W(90^\circ)$  value of 1.47.

These transitions account for 0.43 photons per fission. Assuming that there are eight photons per fission<sup>19</sup> and that the even-even nuclei contribute to  $\frac{1}{4}$  of all the  $\gamma$  rays, we conclude that we measured 22% of the photons associated with even-even fragments. The rest of the transitions are either

statistical transitions leading to the ground-state band or transitions within the ground-state band which were not detected. The latter transitions are expected to have higher anisotropy than the  $2^+ \rightarrow 0^+$  transitions which predominate in our results. The angular distribution of the statistical transitions is not known but, as was indicated in Sec. IV A, has a much less pronounced anisotropy, causing, for example, the reduced anisotropy of the  $2^+ \rightarrow 0^+$  transition with respect to the  $6^+ \rightarrow 4^+$  transition, in  $^{144}\text{Ba}$ .

An estimate of the anisotropy of all the transitions in the ground-state band was obtained by adding separately the contributions of the  $2^+ \rightarrow 0^+$ ,  $4^+ \rightarrow 2^+$ ,  $6^+ \rightarrow 4^+$ , and  $8^+ \rightarrow 6^+$  transitions, according to their relative intensities. In Table III we present the average angular distribution coefficients (calculated from Table I) for the different transitions in the ground-state band and the relative yields of these transitions.<sup>14</sup> The weighted averages of the values given in Table III are  $A_2 = 0.31$  and  $A_4 = -0.09$ , which correspond to a ratio  $W(0^\circ)/W(90^\circ)$  of 1.50.

Table II contains only a small portion of the  $\gamma$  rays associated with the even-odd and odd-odd nuclei. This is because of the large number of transitions deexciting these nuclei. The average  $A_2$  of the transitions in Table II is  $-0.05 \pm 0.02$ . Assuming that these transitions are representative of all the transitions in even-odd and odd-odd fragments and that the statistical transitions in even-even fragments have an isotropic angular distribution, one obtains a value  $N(0^\circ)/N(90^\circ) = 1.07$  for the angular distribution of the gross unresolved spectrum, based on the average ratio 1.50 measured for the ground-state-band transitions in even-even fragments, an average of eight photons per fission,<sup>19</sup> and the assumption that 25% of the  $\gamma$  rays are emitted by even-even fragments. When we compare this value with the value  $N(0^\circ)/N(90^\circ) = 1.11$  obtained by Skarsvag and Singstad,<sup>5</sup> we conclude that most of the anisotropy of the gross spectrum is due to transitions in the ground-state band of the even-even fragments. Therefore the models<sup>28</sup> attempting to derive the magnitude of the primary angular momentum from the anisotropy of the gross spectrum and the statistical properties of all the transitions, without taking into account that a small group of stretched transitions are responsible for most of the anisotropy, may be erroneous. Moreover, since most of the  $\gamma$  rays associated with the ground-state band are below 600 keV, one expects the anisotropy of the gross spectrum below 600 keV to be higher than for the spectrum of higher energies. This in fact was found experimentally by Kandil, El-Mekkawi, and Holub<sup>11</sup> and Lajtai *et al.*<sup>29</sup>



## ACKNOWLEDGMENTS

The authors wish to thank Professor Zeev Fraenkel for very helpful discussions and Dr. J. B. Wilhelmy for kindly providing the statistical calcula-

tions and useful comments. Thanks are also due Mr. Moshe Sidi for electronic support and the instruments workshop of the Weizmann Institute for the design and construction of the experimental chamber.

†This research was supported by a grant from the United States-Israel Binational Science Foundation (B.S.F., Jerusalem, Israel).

\*On leave of absence from the Nuclear Research Center-Negev, P.O.B. 9001, Beer Sheva, Israel.

<sup>1</sup>J. O. Rasmussen, W. Norenberg, and H. J. Mang, Nucl. Phys. A136, 46 (1969).

<sup>2</sup>J. R. Nix and W. J. Swiatecki, Nucl. Phys. 71, 1 (1965).

<sup>3</sup>S. S. Kapoor and R. Ramana, Phys. Rev. 133, B598 (1964).

<sup>4</sup>M. M. Hoffman, Phys. Rev. 133, B714 (1964).

<sup>5</sup>K. Skarsvag and I. Singstad, Nucl. Phys. 62, 103 (1965).

<sup>6</sup>K. Skarsvag, Nucl. Phys. A96, 385 (1967).

<sup>7</sup>G. Graff, A. Lajtai, and L. Nagy, in *Proceedings of the First Symposium on the Physics and Chemistry of Fission, Salzburg, Austria, 1965* (International Atomic Energy Agency, Vienna, 1965), p. 163.

<sup>8</sup>G. V. Val'skii, G. A. Petrov, and Yu. S. Pleva, Yad. Fiz. 5, 734 (1967) [Sov. J. Nucl. Phys. 5, 521 (1967)].

<sup>9</sup>G. V. Val'skii, G. A. Petrov, and Yu. S. Pleva, Yad. Fiz. 8, 297 (1968) [Sov. J. Nucl. Phys. 8, 171 (1969)].

<sup>10</sup>P. Armbruster, F. Hossfeld, H. Labus, and K. Reichelt, in *Proceedings of the Second International Atomic Energy Agency Symposium on the Physics and Chemistry of Fission, Vienna, Austria, 1969* (International Atomic Energy Agency, Vienna, 1969), p. 545.

<sup>11</sup>A. T. Kandil, L. S. El-Mekkawi, and R. Holub, Nucl. Phys. A224, 468 (1974).

<sup>12</sup>J. B. Wilhelmy, E. Cheifetz, R. C. Jared, S. G. Thompson, and H. R. Bowman, Phys. Rev. C 5, 2041 (1972).

<sup>13</sup>J. T. Routti and S. G. Prussin, Nucl. Instrum. Methods 72, 125 (1969).

<sup>14</sup>E. Cheifetz, J. B. Wilhelmy, R. C. Jared, and S. G. Thompson, Phys. Rev. C 4, 1913 (1971).

<sup>15</sup>E. Cheifetz and J. B. Wilhelmy, in *Nuclear Spectroscopy and Reactions* (Academic, New York, 1974), Pt. C, p. 229.

<sup>16</sup>W. John, F. W. Guy, and J. J. Wesolowski, Phys. Rev. C 2, 1451 (1970).

<sup>17</sup>R. G. Clark, L. E. Glendenin, and W. L. Talbert, in *Proceedings of the Third International Atomic Energy Agency Symposium on the Physics and Chemistry of Fission, Rochester, 1973* (International Atomic Energy Agency, Vienna, 1974), Vol. II, p. 221.

<sup>18</sup>J. R. Huizenga and R. Vandenbosch, Phys. Rev. 120, 1305 (1960).

<sup>19</sup>R. W. Peele and F. C. Maienschein, Phys. Rev. C 3, 373 (1971).

<sup>20</sup>J. B. Wilhelmy (private communication).

<sup>21</sup>J. O. Rasmussen and T. T. Sugihara, Phys. Rev. 151, 992 (1966).

<sup>22</sup>L. A. Sliv and I. M. Band, Report 57ICC, Physics Department, University of Illinois, Urbana (unpublished).

<sup>23</sup>S. R. de Groot, H. A. Tolhoek, and W. J. Huiskamp, in *Alpha-, Beta-, and Gamma-Ray Spectroscopy*, edited by K. Siegbahn (North-Holland, Amsterdam, 1965), Vol. 2, p. 1199.

<sup>24</sup>R. L. Watson, J. B. Wilhelmy, R. C. Jared, C. Rugge, H. R. Bowman, S. G. Thompson, and J. O. Rasmussen, Nucl. Phys. A141, 449 (1970).

<sup>25</sup>R. C. Jared, H. Nifenecker, and S. G. Thompson, in *Proceedings of the Third International Atomic Energy Agency Symposium on the Physics and Chemistry of Fission, Rochester, 1973* (see Ref. 17), Vol. II, p. 211.

<sup>26</sup>I. Ragnarsson, in *Proceedings of the International Conference on the Properties of Nuclei far from the Region of Beta-Stability*, Leysin, 1970 (unpublished), Vol. 2, p. 847.

<sup>27</sup>E. Cheifetz, R. C. Jared, S. G. Thompson, and J. B. Wilhelmy, Nuclear Chemistry Annual Report UCRL-20426, 1970 (unpublished), p. 157.

<sup>28</sup>V. M. Strutinskii, Zh. Eksp. Teor. Fiz. 37, 861 (1959) [Sov. Phys.-JETP 10, 613 (1960)].

<sup>29</sup>A. Lajtai, K. Jeki, Gy Kluge, I. Vinnay, F. Engard, P. P. Dyachenko, and B. D. Kuzminov, in *Proceedings of the Third International Atomic Energy Agency Symposium on the Physics and Chemistry of Fission, Rochester* (see Ref. 17), Vol. II, p. 249.